Estimation of indocyanine green concentration in blood from fluorescence emission: application to hemodynamic assessment during hemodialysis

Jean-Michel I. Maarek
University of Southern California
Department of Biomedical Engineering
and
Alfred E. Mann Institute for Biomedical Engineering
Denney Research Center 140
1042 Downey Way
Los Angeles, California 90089

Daniel P. Holschneider
University of Southern California
Departments of Cell and Neurobiology
and
Department of Psychiatry and Biobehavioral Sciences
and
Department of Neurology
and
Department of Biomedical Engineering
and
Alfred E. Mann Institute for Biomedical Engineering
Los Angeles, California 90089

Abstract. There is considerable interest in assessing cardiovascular function noninvasively in patients receiving hemodialysis. A possible approach is to measure the blood concentration of bolus-injected indocyanine green dye and to apply the dye-dilution method for estimating cardiac output and blood volume. Blood ICG concentration can be derived from a measurement of the ICG fluorescence through the dialysis tubing if a simple and unique calibration relationship can be established between transmural fluorescence intensity and blood ICG concentration. We investigated this relationship using Monte Carlo simulations of light transport in blood with varying hematocrit and ICG concentrations and performed empiric measurements of optical absorption and ICG fluorescence emission to confirm our findings. The ICG fluorescence intensity measured at the blood surface, as well as the light intensity remitted by the blood, varied as hematocrit changes modified the absorption and scattering characteristics of the blood. Calibration relationships were developed between fluorescence intensity and ICG concentration that accounted for hematocrit changes. Combining the backreflected fluorescence and the reflected light measured near the point of illumination provided optimal signal intensity, linearity, and robustness to hematocrit changes. These results provide a basis for developing a noninvasive approach to derive optically circulating blood ICG concentration in hemodialysis circuits.
[DOI: 10.1117/1.3233652]

Keywords: indocyanine green; fluorescence; blood; hematocrit; Monte Carlo simulation; cardiac output; blood volume; hemodialysis.

Paper 08256RR received Jul. 26, 2008; revised manuscript received Jul. 13, 2009; accepted for publication Jul. 14, 2009; published online Oct. 12, 2009.

1 Introduction

Intradialytic hypovolemia and the ensuing hypotension complicates up to 20% of hemodialysis treatments,[1] which has generated considerable interest in developing practical methods for quantitative assessment of hemodynamic parameters, including cardiac output, stroke volume, and circulating blood volume during hemodialysis.[2,3] Notably, Mitra et al.[4] demonstrated that absolute values of the plasma volume and circulating blood volume could be determined during hemodialysis from spectrophotometric measurements of indocyanine green (ICG) concentration in arterial blood samples obtained at repeated time intervals a few minutes after a bolus injection of the ICG dye. Blood volume estimates obtained in this fashion reflected decreases of the circulating blood volume during hemodialysis and ultrafiltration. While this method provides useful information for patient monitoring and clinical understanding of intradialytic hypotension, its implementation is limited by the need for repeated blood sampling and spectrophotometric measurements of ICG concentration in plasma samples that are time consuming and tedious. A more widespread adoption would be facilitated by technology that enabled direct measurement of the ICG concentration transmurally through the translucent plastic tubes leading from the patient to the dialysis machine.

Transcutaneous measurements of circulating blood ICG concentration have been described using optical absorption[5] or optical fluorescence[6,7] of the ICG dye at selected near-infrared wavelengths and applied to estimate cardiac output and circulating blood volume in experimental animals and humans in various clinical settings.[7–9] Similar techniques could in principle be applied to measure blood ICG concentration through the wall of the hemodialysis tubing. Ideally, a unique calibration relationship would relate the concentration of ICG circulating in the dialysis tube to an optical measurement obtained through the wall of the tube.

For such a measurement, a substantial benefit of deriving the blood ICG concentration from fluorescence as opposed to

Address all correspondence to: Jean-Michel Maarek, Department of Biomedical Engineering, University of Southern California, 1042 Downey Way, Denney Research Center 140, Los Angeles, CA 90089-1111. Tel: (213) 740 0346; Fax: (213) 821 3897; E-mail: maarek@usc.edu

1083-3668/2009/14(5)/054006/12/$25.00 © 2009 SPIE

optical absorption measurements lies in the fact that there is no endogenous source of fluorescence at the near-infrared wavelengths at which ICG fluoresces (peak fluorescence at 830 nm). Conversely, the optical absorption of ICG (peak absorption at 805 nm) overlaps with the absorption of the far more abundant blood hemoglobin. Large amounts of ICG (5 to 20 mg) must be injected in adult humans to create an appreciable change of the optical absorption and transcutaneously detect useful ICG absorption curves.[10] In contrast, well-defined fluorescence dilution curves can be measured through the skin with a much smaller (1 mg) dose of the dye.[7] Given that the half-time of circulating ICG in human subjects is ~3 to 4 min, decreasing the ICG dose increases the rate at which the measurements can be repeated.

Blood hematocrit increases during hemodialysis and ultrafiltration as fluid is removed from the vascular space, which has been used to evaluate relative changes of the circulating blood volume.[2] An increase of the blood hematocrit modifies the optical properties of blood, and particularly its absorption coefficient.[11] The relationship between the fluorescence intensity and the ICG concentration in blood (near linear for ICG concentrations $<2.0\times10^{-3}$ g/L)[12,13] depends in part on the optical properties of the blood. Variations of the optical properties of blood associated with hemoconcentration during ultrafiltration could modify the intensity of the fluorescence signal reaching the transmural photodetection system. The extent to which changes in blood hematocrit affect the fluorescence intensity of circulating ICG measured with an external photodetector is not well understood. Furthermore, the hemodialysis environment allows for detection of the fluorescence of ICG, either from the same side as the illumination source (retroreflected or back-fluorescence) or from the opposite side (transmitted or forward-fluorescence). It is not clear whether either of these signals is more suitable to calibrate the fluorescence intensity as a function of blood ICG concentration while taking into account hematocrit changes associated with ultrafiltration.

In this study, we investigated the relationship between ICG concentration in blood and ICG fluorescence intensity measured at the boundary of the blood medium. The goal was to derive a calibration method that accounted for blood hematocrit changes and could be applied for the quantitative assessment of circulating blood ICG concentration, cardiac output, and circulating blood volume in subjects undergoing hemodialysis. We used the Monte Carlo method[14] to simulate the fluorescence of ICG in blood with different hematocrit levels. ICG fluorescence intensities obtained at different radial distances from the entry point of the excitation beam allowed us to define optimal design criteria for the fabrication of an optical probe for the transmural detection of ICG fluorescence through dialysis tubing. Results of the simulations were compared to empiric *in vitro* measurements of ICG fluorescence in circulating blood with different hematocrit levels.

We showed that by measuring the intensity of the excitation light transmitted through or reflected by the blood, variations of the fluorescence signal with hematocrit could be corrected to produce a calibration relationship between fluorescence intensity and ICG concentration that was unaffected by hematocrit changes.

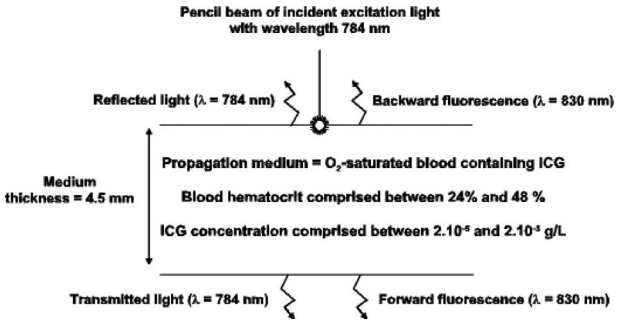

Fig. 1 Blood medium for Monte Carlo simulation. Photons incident on the blood slab at the origin of the axes were tracked as they scattered in the medium. The probability for a photon to become fluorescent increased as the ICG concentration increased. Fluorescent and excitation photons that escaped out of the slab were tabulated based on the distance between the exit point and the axis of cylindrical symmetry of the model represented by the direction of illumination.

2 Methods

2.1 *Simulation of Light Transport and Fluorescence in Blood Tube Model*

2.1.1 *Description of simulation*

Light transport in an infinitely wide blood slab (Fig. 1) with different blood hematocrit levels (Hct) and containing fluorescent ICG in varying concentrations (C_{ICG}) was simulated using the Monte Carlo method.[14,15] Fluorescence was mimicked following the approach of Hyde et al.[16] Briefly, the probability of survival of an excitation photon at each interaction was assumed to be $p=(\mu_s+\mu_{a,ICG})/(\mu_s+\mu_{a,ICG}+\mu_a)$, where μ_s and μ_a represent the scattering and absorption coefficients of the blood medium, and $\mu_{a,ICG}$ is the absorption coefficient of ICG. The "weight" of the excitation photon was reduced by a factor p at each interaction event. Furthermore, at each interaction, the excitation photon was either scattered in a new direction with probability $p_s=\mu_s/(\mu_s+\mu_{a,ICG})$ or transformed into a fluorescent photon with probability $p_f=\mu_{a,ICG}/(\mu_s+\mu_{a,ICG})$. The photon direction after a scattering event was chosen from a probability distribution described by a Henyey-Greenstein phase function defined by the mean cosine of scattering angle (g).[15] When an excitation photon was transformed into a fluorescent photon, the new photon direction was chosen at random, assuming isotropy of the fluorescence. Fluorescent photons were then tracked with the traditional Monte Carlo scheme, which at each interaction reduced the photon weight by $(\mu_s)/(\mu_s+\mu_{a,ICG}+\mu_a)$. A unit quantum yield for the fluorescence was used, which was of no consequence for the analysis of the change of the fluorescence signals with C_{ICG} and Hct.

A pencil beam of excitation light reached the propagation medium, at the origin of the axes in the direction normal to the plane of the slab (Fig. 1). Reflected light and back-fluorescence emerged from the blood medium on the side illuminated by the excitation beam, while transmitted light and forward-fluorescence emerged after crossing the blood slab. The contribution of photons exiting the blood slab was quantified in bins 0.1 mm wide defined by the distance between the locus of emergence and the origin of the axes, taking into account the cylindrical symmetry of the model. All photons

Table 1 Optical parameters used in the simulation at the wavelengths of illumination (784 nm) and ICG fluorescence excitation (830 nm): absorption coefficient of ICG for a blood ICG concentration 1 g/L ($\mu_{a,ICG,0}$); absorption coefficient ($\mu_{a,b,0}$) and scattering coefficient ($\mu_{s,b,0}$) of blood for a blood hemoglobin concentration of 1 g/L; mean cosine of scattering angle of blood (g). The blood coefficients are for oxygen-saturated blood. Parameters were derived from published data (Refs. 17 and 18).

Coefficient	λ=784 nm	=830 nm
Absorption coefficient of ICG: $\mu_{a,ICG,0}$ (L/g/mm)	38.105	34.061
Absorption coefficient of blood: $\mu_{a,b,0}$ (L/g/mm)	0.00261	0.00348
Scattering coefficient of blood: $\mu_{s,b,0}$ (L/g/mm)	0.417	0.417
Mean cosine of scattering angle of blood: g	0.99	0.99

exiting within the width of the bin were tabulated, irrespective of the angle between the photon direction and the direction normal to the blood slab. Photons at the excitation wavelength (wavelength = 784 nm) and fluorescent photons (wavelength = 830 nm) were tabulated separately. The tally represented the radially resolved reflected light, transmitted light, back-fluorescence, and forward-fluorescence signals. These estimates were divided by the number of photons injected and by the area of the annulus with radius equal to the distance (d) between the center of the bin and the locus of incidence of the excitation beam to determine the throughput, defined as the probability per unit area, for each light signal.[15] The throughputs were noted $R(d)$ (reflected light), $T(d)$ (transmitted light), $BF(d)$ (back-fluorescence), and $FF(d)$ (forward-fluorescence). Each simulation followed the trajectories of 1.5×10^6 photons injected in the medium. The thickness of the blood slab was set at 4.5 mm, a common diameter for hemodialysis tubing. The simulations neglected the influence of the tubing material on the optical signals because such a tubing is near-transparent at the visible and near-infrared wavelengths of interest (between 750 and 850 nm).

2.1.2 *Optical properties of propagation medium*

Different values were used in the simulations (Table 1) for the absorption coefficients of blood μ_a and ICG $\mu_{a,ICG}$ depending on whether tracking a 784-nm excitation photon or an 830-nm fluorescence photon.[17,18] The scattering coefficient of blood μ_s and the mean cosine of scattering angle g were held constant since these parameters vary little between 784 and 830 nm.[11] The optical coefficients of blood were computed as the product of the hemoglobin concentration C_{Hb} (in g/L) and the optical coefficients of oxygen-saturated blood for a hemoglobin concentration of 1 g/L ($\mu_{a,b,0}$ and $\mu_{s,b,0}$; Table 1). Hemoglobin concentration C_{Hb} (in g/L) was calculated as 333* Hct (i.e., C_{Hb}=120 g/L when Hct = 36%). In this way, changing the hematocrit between simulation runs affected both the absorption and the scattering coefficients of the blood medium.[11]

The absorption coefficient of ICG was the product of the ICG concentration C_{ICG} (in g/L) and the absorption coefficient of ICG for a blood ICG concentration of 1 g/L ($\mu_{a,ICG,0}$).[19] The refractive index of the medium was set at 1.37 (Ref. 18).

2.1.3 *Analysis of simulation results*

The back-fluorescence, forward-fluorescence, reflected light, and transmitted light throughputs $BF(d)$, $FF(d)$, $R(d)$, and $T(d)$ were represented as a function of radial distance d to characterize the effect of distance on these quantities for different values of Hct and C_{ICG}. The effects of Hct and C_{ICG} on the throughtputs measured in close proximity or at a distance from the entry point of incident light were also identified. The throughputs $BF(d)$, $FF(d)$, $R(d)$, and $T(d)$ were summed over a 0.5-mm distance to calculate integrated throughputs $\overline{BF}$, $\overline{FF}$ $\bar{R}$ and $\bar{T}$. Two starting points for summation of the throughputs were investigated: proximal to the point of illumination (BF and R summed from d=0.3 to 0.8 mm, noted $\overline{BF}_{0.3}$ and $\bar{R}_{0.3}$; FF and T summed from d=0 to 0.5 mm, noted $\overline{FF}_{0.0}$ and $\bar{T}_{0.0}$) and distal from the point of illumination (BF, R, FF, and T summed from d=2 to 2.5 mm, noted $\overline{BF}_{2.0}$, $\bar{R}_{2.0}$, $\overline{FF}_{2.0}$, and $\bar{T}_{2.0}$, respectively). Note that a 0.3-mm distance was skipped when summing throughputs BF and R to match physical situations requiring a physical separation between the illumination and the detection systems.

This analysis suggested functional forms for the calibration equations used to calculate the ICG concentration C_{ICG} as a function of the measured light signals and that accounted for variations of Hct:

$$C_{ICG} = A \cdot \overline{BF} \cdot \bar{T}^{\alpha}, \tag{1}$$

$$C_{ICG} = B \cdot \overline{FF} \cdot \bar{T}^{\beta}, \tag{2}$$

$$C_{ICG} = D \cdot \overline{BF} \cdot \bar{R}^{\delta}, \tag{3}$$

$$C_{ICG} = E \cdot \overline{FF} \cdot \bar{R}^{\varepsilon}. \tag{4}$$

Each model equation assumed that the fluorescence signal (back-fluorescence or forward-fluorescence) and the ICG concentration varied in direct proportion, which is found empirically for blood ICG concentrations <1 to 2×10^{-3} g/L (Refs. 12 and 20) The transmitted light or the reflected light throughput operated as a correction term that accounted for the effect of the hematocrit and self-absorption of the ICG emission on the proportionality relationship between fluorescence and ICG concentration. In each equation, scaling factors A, B, D, and E and exponents α, β, δ, and ε were determined by minimizing the sum of squared relative differences between the ICG concentrations and the model predictions:

$$\sum \left(\frac{C_{ICG,predicted} - C_{ICG}}{C_{ICG}} \right)^2. \tag{5}$$

Comparison between the models was based on the residual mean squared relative error and the average relative residual

error between the actual and predicted concentrations. All calculations were performed using SPSS (version 11, SPSS, Inc., Chicago).

Thirty simulation runs were performed in all. The ICG concentration C_{ICG} varied in six increments between 2×10^{-5} and 2×10^{-3} g/L to cover the range of circulating ICG concentrations observed empirically in our studies.[6,7] The hematocrit Hct varied in five increments between 24% and 48% (C_{Hb} between 80 and 160 g/L).

2.2 *Empiric Validation*

2.2.1 *Experimental measurements*

Back-fluorescence, forward-fluorescence, reflected, and transmitted light intensities were measured in circulating blood with different hematocrit levels for varying ICG concentrations. Citrated bovine blood (Sierra for Medical Science, Whittier, California, ~3% citrate) was examined in a segment of transparent frothed plastic dialysis tube (4.5-mm ID, 6.5-mm OD) stabilized inside a groove within a cylindrical black metal holder (40 mm outer diameter). Two custom-designed fiber optic probes secured in the metal holder (Ocean Optics, Dunedin, Florida) illuminated the blood in the tube and retrieved the optical signals. One probe bore a 100-μm UV silica fiber that forwarded the excitation light beam to the blood in the tube. The light reflected by the blood was sampled with twenty-three 100-μm fibers arranged within an inner annulus (0.35 to 0.50 mm radius) around the illumination fiber. The back-fluorescence was captured by means of twenty-nine 100-μm fibers arranged in an outer annulus (0.50 to 0.75 mm radius) around the reflected light fibers. On the opposite side of the illumination beam across the blood tube, the second probe bore one hundred and twenty-eight 100-μm fibers arranged within in a circle (0.50 mm outer radius) and randomly divided in equal bundles (64 fibers each) to capture the transmitted light and forward-fluorescence signals. In both probes, the fiber tips were in tight contact with the outer wall of the blood tube.

A temperature-controlled 785-nm diode laser system (Fermion 1, Micro Laser Systems, Garden Grove, California) was coupled to the excitation fiber optic. Four photomultiplier modules (H5784-20, Hamamatsu, Bridgewater, New Jersey) with extended near-infrared response were connected to the fiber bundles to quantify the light signals retrieved from the blood tube. Bandpass interferential filters (Melles Griot, Carlsbad, California) were securely held with metal holders in front of the photomultiplier windows for wavelength selection (reflected and transmitted light: center wavelength = 780 nm; back- and forward-fluorescence: center wavelength = 830 nm). The voltage outputs of the photomultiplier modules were amplified with four lock-in amplifiers (SR 810 and SR 530, Stanford Research Systems, Sunnyvale, California) and recorded with an eight-channel A/D converter module (Powerlab, AD Instruments, Colorado Springs). The laser output power (~4 mW average) was modulated at 1 kHz (~2-mW RMS rectified sine wave) by the reference oscillator signal in one of the lock-in amplifiers.

Blood samples with different hematocrits were obtained by mixing the bovine blood with either plasma or concentrated red blood cells obtained by centrifugation. The blood was circulated in the dialysis tube segment using a peristaltic pump (Masterflex, L/S, Cole-Parmer, Vernon Hills, Illinois) in a closed loop configuration. A reservoir held 120 ml of blood, which was pumped at a rate of 200 ml/min through the tube. ICG (Akorn, Inc., Buffalo Grove, Illinois) from a 50 μg/ml stock solution (in 5% dextrose aqueous solution) was rapidly injected in 800-μl increments (40-μg dose) from a side port and passed through a mixing chamber fabricated from the drip chamber of an intravenous infusion set before reaching the segment of tube in the probe holder. After each injection, the optical traces presented the traditional rapid rise and fall patterns characteristic of indicator dilution traces and reached a plateau that corresponded to the steady-state concentration of the ICG in blood after each incremental dose. Readings of the optical intensities were obtained 3 min after each addition of ICG, when the optical signals had become stable.

The signals measured with the fluorescence fiber bundles prior to the first addition of ICG represented leakage of the excitation light through the 830-nm filters and were used as baseline levels for the steady-state back-fluorescence and forward-fluorescence readings. After the ICG additions had been completed ($0<C_{ICG}<2.5\times10^{-3}$ g/L), the blood was discarded. The circuitry was abundantly rinsed with distilled water before adding blood with a different hematocrit and repeating the measurement sequence. The experiments were repeated twice, and the measured signals were combined to analyze the measured data.

2.2.2 *Analysis of experimental data*

The steady-state reflected light, transmitted light, forward-fluorescence and back-fluorescence measurements obtained 3 min after each serial addition of ICG were evaluated in terms of their ability to predict the blood ICG concentration with equations similar to Eqs. (1)–(4) earlier. The experimental coefficients were determined by minimizing the sum of squared relative differences between the empiric ICG concentrations and the model predictions. Comparison between the models was based on the residual mean squared relative error and the mean relative residual error between the actual and predicted concentrations.

For each blood hematocrit level, the time-varying optical signals recorded while the dye bolus passed in front of the measurement optics were converted to concentration readings using the derived model equations. Only the time-varying signals measured at the time of the first two ICG injections were used such that the starting ICG concentration in the blood was 0 or near 0. The concentration curves obtained after acute ICG injection were processed using previously described algorithms[6] to estimate the pump flow rate and the volume of blood in the circuitry. The estimates were compared with the actual values of the flow rate and blood volume.

3 Results

3.1 *Simulations: Variations of Signal Intensities as a Function of Lateral Distance and Hematocrit*

The back-fluorescence and reflected light throughputs $BF(d)$ and $R(d)$ decreased 35-fold and 15-fold, respectively, as a function of distance d over the first 0.5 mm measured from the locus of illumination [Figs. 2(a) and 2(b)]. The throughputs decreased more gradually and approximately exponentially (linear trend on the semilogarithmic plots of Fig. 2)

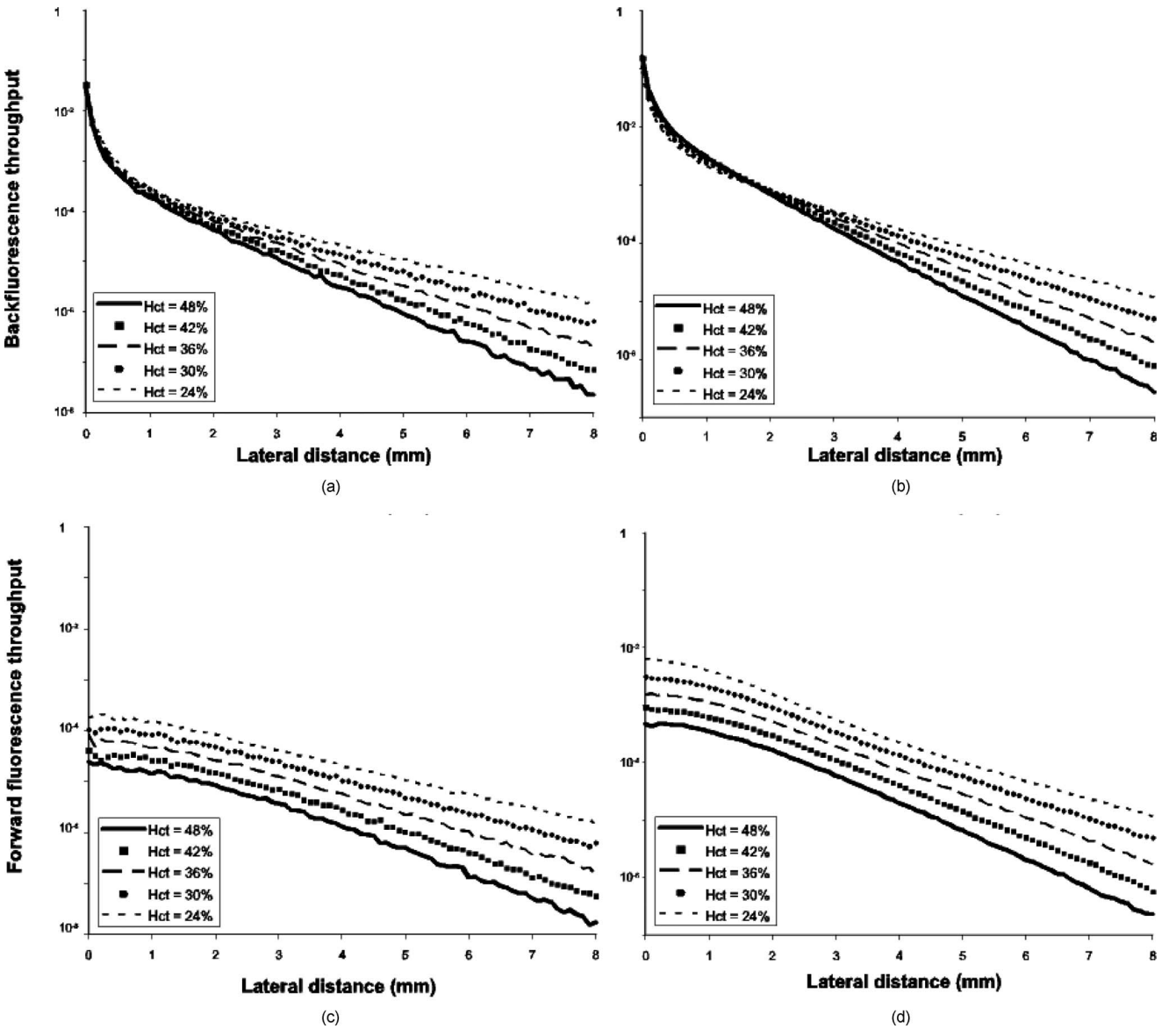

Fig. 2 Probability of emergence per unit area (throughput) as a function of distance between the direction of illumination and the locus of emergence for back-fluorescence (a), reflected light (b), forward-fluorescence (c), and transmitted light (d) when the blood ICG concentration is 10^{-4} g/L. The spread between the traces obtained for different hematocrit levels near the illumination axis (distance <1 mm) is much smaller for the back-fluorescence and reflected light throughputs when compared to the forward-fluorescence and transmitted light throughputs. Near the illumination axis, changing the hematocrit had a smaller effect on the signals measured on the same side of the slab as the illumination beam but changed substantially for the signals measured on the opposite side.

starting from $d \sim 1.5$ mm. Increasing the hematocrit resulted in a diminution of $BF(d)$ at all distances d [Fig. 2(a)]. In contrast, increasing the hematocrit increased $R(d)$ for $d < 1.5$ mm but decreased $R(d)$ for $d > 1.5$ mm [Fig. 2(b)].

Contrasting with the decay of $BF(d)$ and $R(d)$ observed for small values of d, the forward-fluorescence and transmitted light throughputs $FF(d)$ and $T(d)$ were approximately unchanged for $d < 1$ mm [Figs. 2(c) and 2(d)]. For $d > 1$ mm, the throughputs $FF(d)$ and $T(d)$ decreased exponentially with d. Increasing the hematocrit Hct reduced $FF(d)$ and $T(d)$ in an approximately exponential fashion. Importantly, $FF(d)$ measured near the illumination axis was much more sensitive to hematocrit changes than $BF(d)$.

3.2 *Simulations: Variations of Integrated Throughputs as a Function of ICG Concentration and Hematocrit*

The integrated back-fluorescence throughputs $\overline{BF}_{0.3}$ and $\overline{BF}_{2.0}$ increased with C_{ICG} [Figs. 3(a) and 4(a)]. The increase was near linear for $C_{ICG} < 10^{-3}$ g/L. The slope $\Delta\overline{BF}/\Delta C_{ICG}$ diminished for $C_{ICG} > 10^{-3}$ g/L, minimally for $\overline{BF}_{0.3}$, but markedly for $\overline{BF}_{2.0}$. Throughput $\overline{BF}_{2.0}$ was more sensitive to Hct changes and decreased by ~50%, whereas $\overline{BF}_{0.3}$ decreased by ~30% when Hct increased in agreement with the trends noted on the back-fluorescence profile as a function of lateral distance d [Fig. 2(a)].

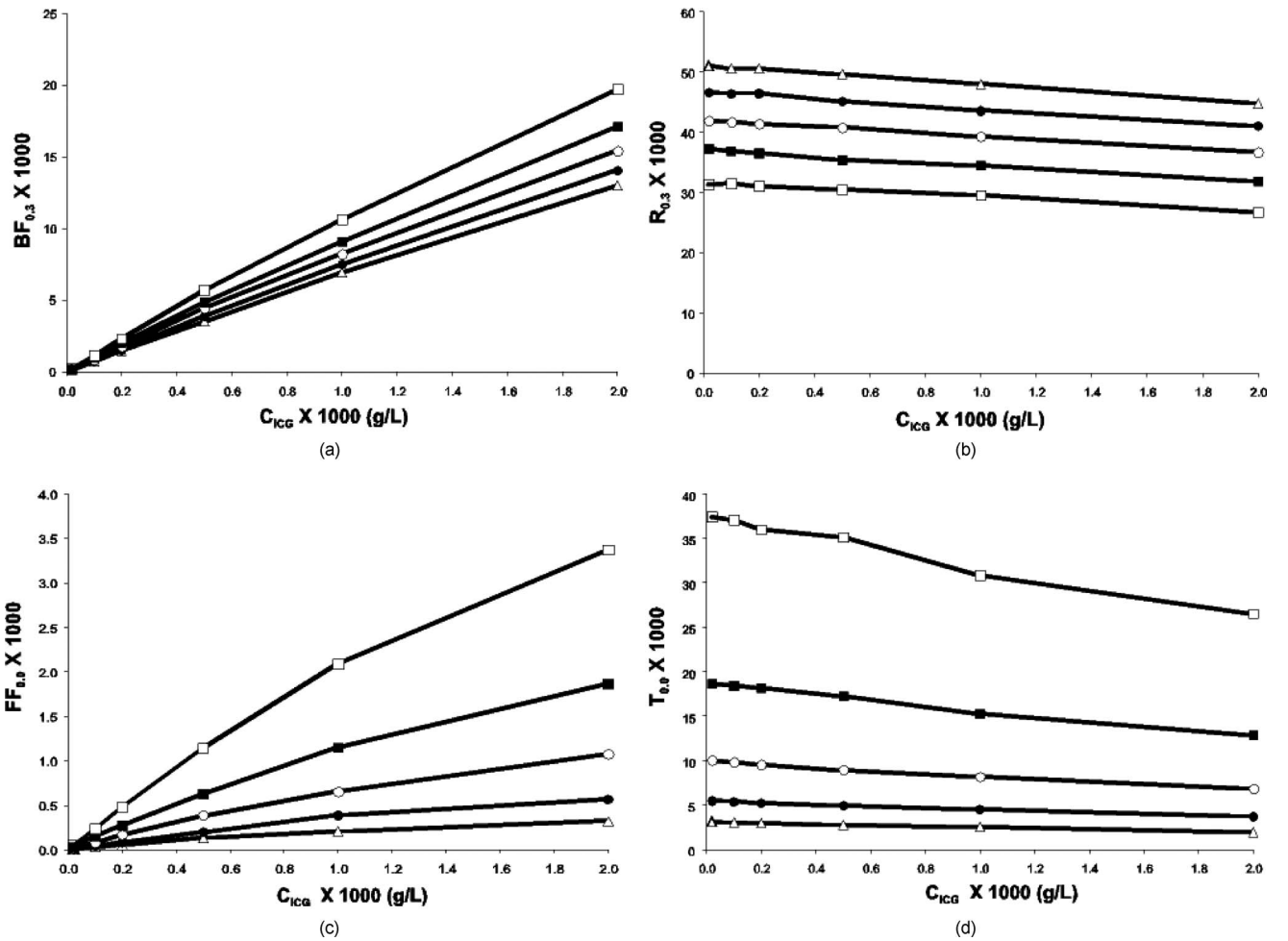

Fig. 3 Simulated back-fluorescence (a), reflected light (b), forward-fluorescence (c), and transmitted light throughputs (d) measured near the illumination axis as a function of blood ICG concentration (C_{ICG}) for different hematocrits (□: 24%; ■: 30%; ○: 36%; ●: 42%; △: 48%). The throughputs were integrated over a 0.5-mm-wide annulus whose inner radius was 0.3 mm for the back-fluorescence and reflected light and 0.0 mm for the forward-fluorescence and transmitted light.

The integrated reflected light throughputs $\bar{R}_{0.3}$ [Fig. 3(b)] and $\bar{R}_{2.0}$ [Fig. 4(b)] decreased when C_{ICG} increased. Reflectance throughput $\bar{R}_{0.3}$ increased in near-equal steps when Hct increased for all ICG concentrations, In contrast, reflectance throughput $\bar{R}_{2.0}$ decreased when Hct increased, with little change being observed for Hct $\leqslant$ 36% and more substantial decreases for higher hematocrits. The summation distance (2.0 to 2.5 mm) for calculating $\bar{R}_{2.0}$ was near the distance range where the curves $R(d)$ calculated for different values of Hct intersect [Fig. 2(b)], giving rise to this complex trend.

Integrated forward-fluorescence throughputs $\overline{FF}_{0.0}$ and $\overline{FF}_{2.0}$ increased near linearly as a function of C_{ICG} only for $C_{ICG} \leqslant 10^{-3}$ g/L [Figs. 3(c) and 4(c)]. Increasing the hematocrit reduced both forward-fluorescence throughputs in a near-exponential fashion as noted on the forward-fluorescence profile as a function of d [Fig. 2(c)].

Integrated transmitted light throughputs $\bar{T}_{0.0}$ and $\bar{T}_{2.0}$ decreased as a function of C_{ICG} [Figs. 3(d) and 4(d)]. The slope of the decrease was less when the hematocrit was larger. Increasing the hematocrit reduced the transmittance throughputs for all ICG concentrations in a near-exponential fashion.

3.3 *Simulations: Evaluation of ICG Calibration Equations*

Table 2 summarizes the optimal values of the scaling factors and exponents for estimating C_{ICG} from the optical measurements based on the model equations (1)–(3). [Eq. (4)] could not describe the variations of C_{ICG} satisfactorily.] We noted that for all values of C_{ICG}, increasing Hct decreased the back-fluorescence throughput and the transmitted light throughput. For Eq. (1), the negative value of exponent α amounted to multiplying the decreasing back-fluorescence signal by a correction factor that increased with Hct [$A \cdot \bar{T}_{0.0}^{\alpha}$ or $A \cdot \bar{T}_{2.0}^{\alpha}$), resulting in a near-linear dependence of C_{ICG} on $\overline{BF}_{0.3}$ or $\overline{BF}_{2.0}$. A similar observation accounted for the negative value of exponent β in Eq. (3). In contrast, increasing Hct increased the reflected light throughput $\bar{R}_{0.3}$. The factor $(D \cdot \bar{R}_{0.3}^{\delta})$ with a positive value of δ in Eq. (3) increased and compensated for the diminishing value of $\overline{BF}_{0.3}$. Overall, Eq. (1), with the back-fluorescence and transmitted light throughputs measured

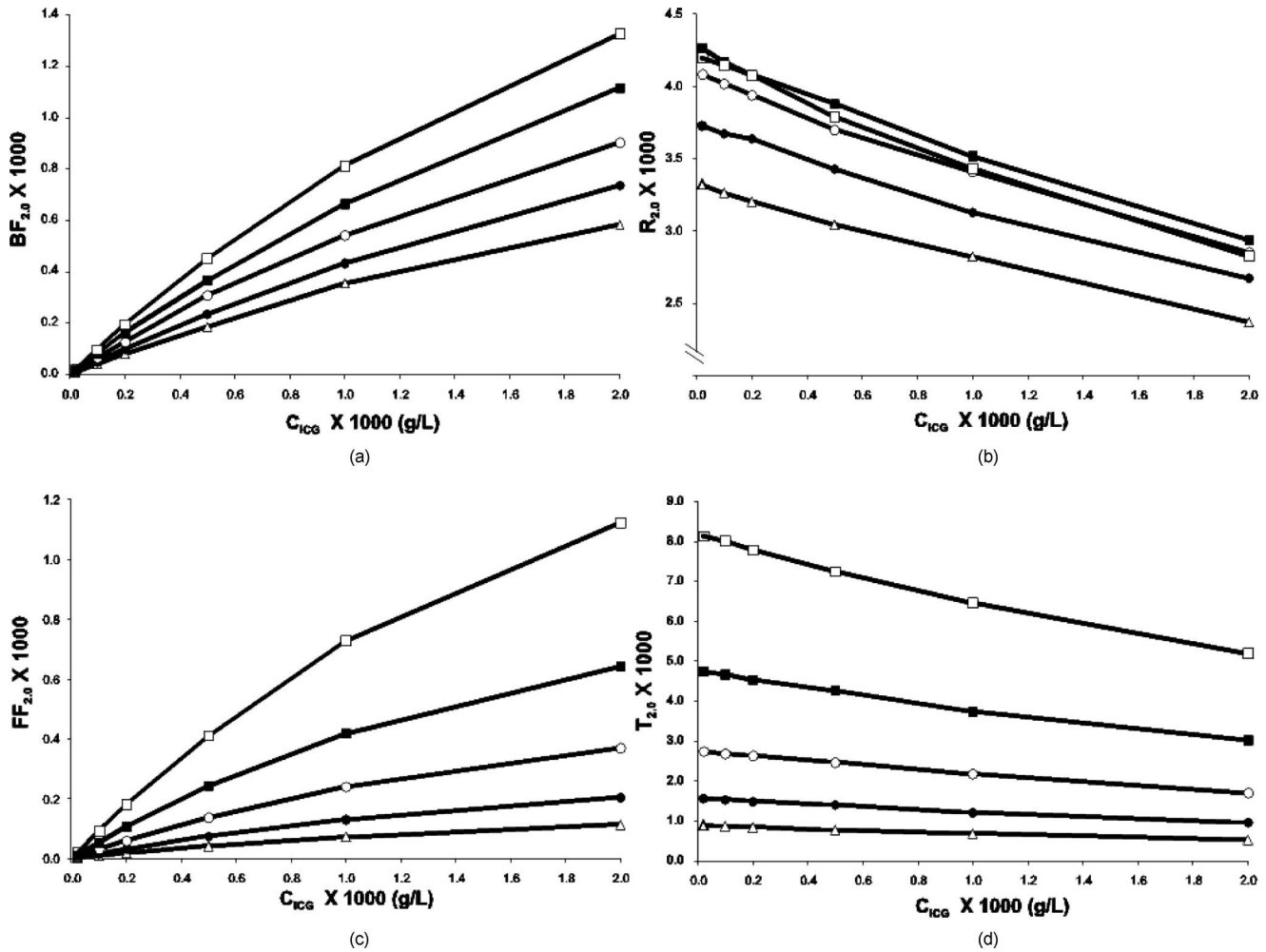

Fig. 4 Simulated back-fluorescence (a), reflected light (b), forward-fluorescence (c), and transmitted light throughputs (d) measured away from the illumination axis as a function of blood ICG concentration (C_{ICG}) for different hematocrits (□: 24%; ■: 30%; ○: 36%; ●: 42%; △: 48%). The throughputs were integrated over a 0.5-mm-wide annulus whose inner radius was 2 mm. Note that the back-fluorescence intensity is ~20 times less intense than that measured near the illumination axis [Fig. 3(a)], while the forward-fluorescence intensity is reduced only by a factor 3.5 [Fig. 3]. The back-fluorescence response becomes nonlinear for ICG concentrations $>10^{-3}$ g/L.

near the illumination point, and Eq. (2), with the forward-fluorescence and transmitted light throughputs measured at a distance from the illumination axis, resulted in the smallest residual errors.

3.4 *Empiric In Vitro Measurements of Optical Signals*

Variations of the experimental optical signals with blood ICG concentration and with blood hematocrit reflected the trends predicted from the simulations. Back-fluorescence increased near-linearly with C_{ICG}, with a slightly reduced slope for the higher values C_{ICG} [Fig. 5(a)]. For the same value of C_{ICG}, the back-fluorescence intensity was more intense when Hct was reduced. The reflected light intensity decreased slightly and gradually when C_{ICG} increased [Fig. 5(b)]. Reflected light intensity decreased when hematocrit decreased, but the decreasing trend was not as gradual as that observed in the simulations [Fig. 3(b)]. Small position shifts in replacing the blood tube in its holder after each rinse could have affected more acutely the reflected light signal than the other measurements since the reflected light was measured over the narrowest surface area very near the illumination fiber.

Forward-fluorescence [Fig. 5(c)] increased with C_{ICG}, presenting larger variations with Hct when compared to back-fluorescence, in agreement with the simulation results. Last, transmitted light intensity was strongly dependent on Hct and decreased gradually with C_{ICG} [Fig. 5(d)].

Experimental observations from two separate blood loop experiments were combined to estimate the parameters of Eqs. (1)–(3) applied to the experimental measurements. The exponents for model equations (1)–(3) ($\alpha = -0.26$, $\beta = -0.99$, $\delta = 0.99$) were similar to their counterparts determined from the analysis of the simulation results (Table 2). Notably, parameter α, derived from experimental measurements obtained from a distance of 0.8 mm from the illumination center, was between -0.18 and -0.40, the values obtained in the simulations by integration over the 0.3 to 0.8 mm and 2.0 to 2.5 mm ranges of distance from the illumination beam, respectively. Equation (3) was as accurate as Eq. (2) and only slightly less accurate than Eq. (1) with respect to estimating the circulating ICG concentration.

Table 2 Mean value ± standard error for the estimated coefficients (scaling factors A, B, D; exponents α, β, δ) of the model calibration equations as estimated from the simulations or derived experimentally. In the simulations, parameters (BF_i, FF_i, R_i, and T_i) represented the back-fluorescence, forward-fluorescence, reflected light, and transmitted light throughputs (probability of photon emergence per unit area) measured near the axis of illumination ($i=0.0, 0.3$) or at a 2-mm distance ($i=2.0$). Parameters BF_{exp}, FF_{exp}, R_{exp}, and T_{exp} designated the corresponding experimental signals. The quality of the fit was evaluated from the mean squared residual error and the average relative residual error between the data and the value predicted by the model: $|(C_{ICG,predicted}-C_{ICG})/C_{ICG}|$. The experimental measurements were repeated on different days with slightly different equipment settings. The experimental results were combined to fit the data to the model equations and determine a single best-fit exponent while allowing for different scaling factors for the two data sets. Note that Eq. (4) could not describe the variations of C_{ICG} satisfactorily when used to approximate the data (simulated or experimental) with the model equation.

Model equation	Scaling factor (A, B, D)	Exponent (α, β, δ)	Mean squared residual error	Average relative residual error (%)
1 ($C_{ICG}=A\cdot\overline{BF_{0.3}}\cdot\overline{T_{0.0}}^{\alpha}$)	0.049±0.001	−0.181±0.006	0.001	2.8
1 ($C_{ICG}=A\cdot\overline{BF_{2.0}}\cdot\overline{T_{2.0}}^{\alpha}$)	0.149±0.013	−0.404±0.014	0.004	5.3
1 ($C_{ICG}=A\cdot\overline{BF_{exp}}\cdot\overline{T_{exp}}^{\alpha}$)	$4.614\pm002\times10^{-3}$ $2.600\pm002\times10^{-3}$	−0.260±001	0.011	8.6
2 ($C_{ICG}=B\cdot\overline{FF_{0.0}}\cdot\overline{T_{0.0}}^{\beta}$)	0.020±0.002	−0.903±0.023	0.005	5.8
2 ($C_{ICG}=B\cdot\overline{FF}_{2.0}\cdot\overline{T_{2.0}}^{\beta}$)	0.007±0.001	−1.037±0.006	0.001	2.0
2 ($C_{ICG}=B\cdot\overline{FF}_{exp}\cdot\overline{T_{exp}}^{\beta}$)	$8.283\pm0.006\times10^{-4}$ $4.095\pm0.004\times10^{-3}$	−0.993±0.001	0.019	12
3 ($C_{ICG}=D\cdot\overline{BF}_{0.3}\cdot\overline{R_{0.3}}^{\delta}$)	1.491±0.421	0.794±0.087	0.008	7.3
3 ($C_{ICG}=D\cdot\overline{BF_{2.0}}\cdot\overline{R_{2.0}}^{\delta}$)	NA	NA	NA	NA
3 ($C_{ICG}=D\cdot\overline{BF}_{exp}\cdot\overline{R_{exp}}^{\delta}$)	$1.020\pm0.007\times10^{-3}$ $6.383\pm0.003\times10^{-4}$	0.985±005	0.016	11

The pump flow rate and volume of blood in the circuitry derived from the measured optical signals and Eqs. (1) to (3) (Table 3) differed by less than 10% from the empiric pump rate and blood volume in the circuitry. Thus, the model calibration equations could be used to convert the transient optical changes associated with ICG injections to useful first-pass ICG concentration curves within the framework of indicator-dilution theory.

4 Discussion

4.1 *Effect of C_{ICG} on Integrated Throughputs*

In the simulations, the integrated back-fluorescence and forward-fluorescence throughputs increased near linearly with C_{ICG} only for $C_{ICG}<10^{-3}$ g/L. Several groups reported[12,21] that when the ICG concentration is elevated, its fluorescence emission is partially absorbed by dye molecules in the environment (inner filter effect), resulting in a decreasing slope for the fluorescence intensity versus C_{ICG} relationship. Fluorescent light detected at a large distance from the locus of illumination traveled farther and deeper in the blood medium and was more susceptible to being absorbed by ICG when C_{ICG} was elevated. Thus, the inner filter effect was more noticeable for the forward-fluorescence throughputs detected after traversal of the blood medium when compared to the back-fluorescence throughputs detected on the side of the illumination. For the back-fluorescence throughputs, $\overline{BF}_{2.0}$ was more sensitive to the inner filter effect when compared to $\overline{BF}_{0.3}$. The experimentally measured back-fluorescence and forward-fluorescence intensities largely reflected the inner filter effect and the fact that forward-fluorescence was more sensitive to this effect than back-fluorescence. In addition to the inner filter effect, which was reproduced in the simulations, aggregation of ICG monomers into polymer chains has been reported, which could have reduced the emission yield for high ICG concentrations in the experimental measurements.[20]

The transmitted light and reflected light throughputs decreased when C_{ICG} increased, in agreement with increased absorption of the light traveling through the blood medium by more numerous ICG molecules. Reflected light throughput $\bar{R}_{0.3}$ represented the contribution of photons, which, on average, traveled the least in the medium, and was therefore least dependent on C_{ICG}.

4.2 *Consequences for the Design of an ICG Fluorescence Probe for Hemodialysis Applications*

In the simulations, all fluorescence throughputs were dependent on Hct, which affected the absorption and scattering properties of the propagation medium. Back-fluorescence throughput $\overline{BF}_{0.3}$ estimated near the point of entry of the illumination beam was least affected by hematocrit changes. As

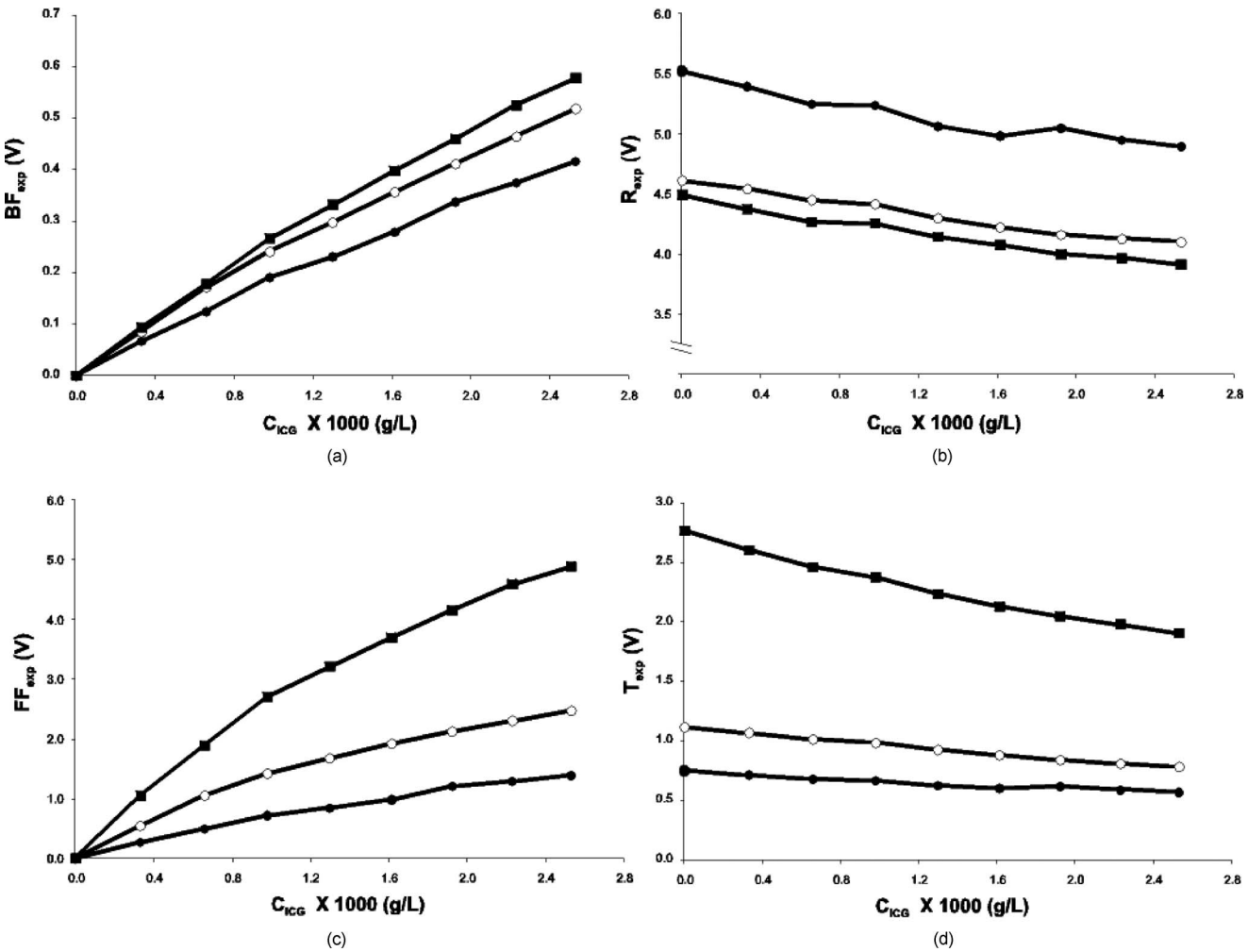

Fig. 5 Back-fluorescence (a), reflected light (b), forward-fluorescence (c), and transmitted light intensities (d) measured experimentally in blood as a function of blood ICG concentration (C_{ICG}) for different hematocrits (■: 28%; ○: 35%; ●: 42%). The trends observed for each signal as ICG concentration and hematocrit changed are in agreement with the simulation predictions. The absolute intensities cannot be compared because the collection optics and the level of amplification were different for back-fluorescence, reflected light, forward-fluorescence, and transmitted light.

Table 3 Empiric volumetric flow rates set by the blood pump and reservoir blood volume compared with the flow rate and blood volume predicted from the optical signals by application of the calibration model equations in Table 2 to the *in vitro* measurements of fluorescence and diffusely scattered excitation light across the blood tube. The empiric volume flow rate was determined by the setting of the Masterflex pump and verified with the "bucket and stopwatch" method by timing the emptying of the circuitry in a graduated cylinder. The empiric volume was that used to fill the priming reservoir of the blood loop with a graduated cylinder. After conversion of the optical measurements to circulating ICG concentrations, the concentration curves were analyzed using the equations from indicator dilution theory (Refs. 5 and 6) to calculate blood flow and reservoir volume.

		Empiric value	Estimate Eq. (1)	Estimate Eq. (2)	Estimate Eq. (3)
Test 1	Pump rate (ml/min)	207	220±20	226±36	214±8
	Volume (ml)	120	112±13	115±22	103[a]±6
Test 2	Pump rate (ml/min)	285	298±31	307±37	300±33
	Volume (ml)	120	123±16	128±17	120±16

[a]Denotes statistical difference from empiric value ($p<0.05$).

noted earlier, $\overline{BF}_{0.3}$ was the fluorescent throughput least dependent on the inner filter effect, and the most intense of those studied in the simulations. These aggregate results suggest that monitoring the back-fluorescence intensity near the illumination point is the most favorable configuration for a measurement probe used to derive circulating ICG concentration based on optical fluorescence measurements.

The throughputs estimated from the simulations corresponded to the signal intensity per unit area detected over an annular window centered on the illumination axis, equivalent to a slit detector, positioned radially with respect to the direction of illumination of the medium. These throughputs must be multiplied by the area of the annuli and integrated along the radial direction to compare the signals measured with circular detectors of different apertures. The calculations show that 48% of all back-fluorescence photons emerge within an aperture of 0.5 mm and 64% within an aperture of 1 mm when the hematocrit is 36%. In contrast, only 6% of all forward-fluorescence photons emerge within an aperture of 0.5 mm and 17% within an aperture of 1 mm for the same hematocrit. Similarly, 33% of all reflected photons exit the medium within 0.5 mm of the illumination axis, while that is true for only 8% of all transmitted photons. Thus, a small-diameter circular detector or fiber optic bundle positioned to measure the back-fluorescence or reflected light intensity captures a large fraction of the available signal. A much larger aperture is necessary to capture a substantial fraction of the available forward-fluorescence or transmitted light. A measurement system designed to capture forward-fluorescence would be ineffective unless it had a large aperture. Such a configuration, however, is limited by the finite diameter of the dialysis tube (~5 mm) and would make the measurement more sensitive to the variability of the interface between the detector and the curvature of the blood tube.

Correcting the back-fluorescence signal for variations associated with the hematocrit may be done using the transmitted light [Eq. (1)] or the reflected light [Eq. (3)]. The transmitted light approach produced slightly more accurate estimates of the ICG concentration both in the simulations and in the experimental tests. Practically, using the reflected light signal for the correction may be more convenient with respect to the construction of the probe since the fiber optic bundles used to measure the two signals could be adjacent rather than facing each other on opposite sides of the blood tube. Measuring the reflected light anywhere between 0 and 1 mm from the illumination axis yields a factor that increases by 60% when the hematocrit increases from 24% to 48% and could be used to account for hematocrit changes.

4.3 *Relation to Previous Work*

Several authors have examined the effect of the medium optical properties on the detected fluorescence emission intensity with the goal of estimating the concentration of a fluorophore in a turbid medium independently of the medium's optical properties.[22–24] In particular, Weersink and colleagues[22] demonstrated that the ratio (back-fluorescence/reflected light) measured at specific distances from the illumination point source was linearly related to fluorophore concentration over a wide range of tissue optical properties. These results were equivalent to those derived in our study for the ratio of forwardfluorescence/transmitted light (coefficient $\beta \sim -1$), but they differed from those we obtained for the (back-fluorescence/reflected light) ratio (coefficient $\delta \sim 0.8$ to 1). The distances from the illumination point at which the optical measurements were obtained were different in our study and in the work of Weersink et al.[22] Furthermore, our study considered a propagation medium equivalent to blood and therefore more absorbent ($\mu_a \sim 0.2$ to 0.4 mm^{-1}) than the tissue phantoms examined in the earlier work ($\mu_a \sim 0.001$ to 0.1 mm^{-1}). It is noteworthy that previous work mostly envisaged fluorescence measurements from the surface of optically thick tissues and organs. Therefore, the use of transmitted excitation light and forward-fluorescence emission was not considered. Our study shows that such quantities would provide useful information if measured from optically thin tissue that can be transilluminated, such as the earlobe or the fingertips.

4.4 *Limitations*

Mention should be made of several limitations of the study. The propagation medium for the simulations was assumed to be semi-infinite, while the experiment were performed with blood contained in a cylindrical plastic tube. The semi-infinite blood slab was chosen for the simulations to characterize the interactions between blood hematocrit, ICG concentration, and optical measurements of fluorescence, transmitted light, and reflected light intensities, independently of a particular shape for the experimental measurement chamber. As indicated in discussing the design of a fluorescence probe, the integrated back-fluorescence and reflected light signals are concentrated near the point of entry of the illumination beam and therefore are less sensitive to the shape of the medium when compared to the forward-fluorescence and transmitted light signals. The simulations assumed an infinitely thin pencil of light whereas the experiments used a 100-μm optic fiber to carry the excitation light to the blood medium. Last, the simulations did not consider absorption, scattering, or refraction in the blood tube. Most plastic materials used for dialysis tubing are near-transparent at visible and near-infrared wavelengths, and their refractive index (~1.35 to 1.55) is close to the refractive index of blood.[18]

Simulations and experimental results were obtained for blood ICG concentrations $C_{ICG} < 2.5 \times 10^{-3}$ g/L. It is known that ICG fluorescence increases linearly only within a limited range of concentrations (< 1 to 2×10^{-3} g/L). Aggregation of ICG monomers into polymer chains reduces the emission yield for higher concentrations.[12,20] It is possible that the proposed model equations would not extend much beyond the range of concentrations examined in the study.

The ICG calibration equations tested on the simulation results considered only combinations of fluorescent quantities and incident light quantities that were both obtained proximal to the axis of illumination or distal from the axis of illumination. Other combinations that mixed proximal and distal measurements (i.e., $BF_{0.3} \cdot T_{2.0}$) were not tested, as these combinations would be less practical to implement.

Blood ICG concentration C_{ICG} estimated using the model equations reproduced accurately the ICG concentration used as a parameter in the Monte Carlo simulations [Fig. 6(a)]. Concentration C_{ICG} predicted from the experimental data us-

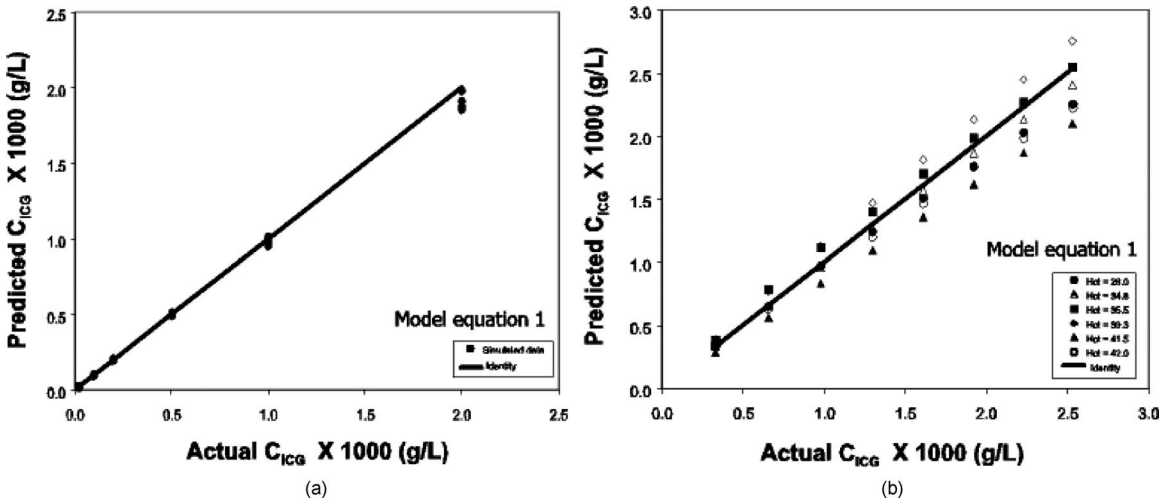

Fig. 6 (a) Blood ICG concentration (C_{ICG}) predicted with Eq. (1) applied to back-fluorescence and transmitted light throughputs ($\overline{BF}_{0.3}$ and $\bar{T}_{0.0}$) as a function of actual C_{ICG} concentration used in Monte Carlo simulation. Symbols: concentration predicted from simulated data; solid line: line of identity. (b) Blood ICG concentration (C_{ICG}) predicted with Eq. (1) applied to back-fluorescence and transmitted light intensities ($\overline{BF}_{exp}$ and $\bar{T}_{exp}$) measured experimentally. Symbols: concentration predicted from experimental data obtained for different values of the hematocrit (Hct); solid line: line of identity. The larger dispersion around the line of identity in the concentrations predicted from the experimental data reflects the larger average relative residual error for the experimental data (8.6% versus 2.8%; Table 2).

ing the model equations was more spread out around the line of identity [Fig. 6(b)]. The variability of the prediction was not related to the hematocrit, suggesting that the effect of Hct on the predicted C_{ICG} had been accounted for by the model. Rather, the spread of the predicted C_{ICG} more noticeable for the higher ICG concentrations likely reflected experimental errors and the fact that the minimization approach used to estimate the parameters of the model was carried out on the sum of relative differences between the model predictions and C_{ICG}. This approach was chosen to increase the contribution of the low values of C_{ICG} in the selection of the model parameters. In the intended application of estimating cardiac output and circulating blood volume using fluorescence dilution methods,[6] concentrations $< 20\%$ of the maximum circulating C_{ICG} (~ 1 to 2×10^{-3} g/L) are the most important to estimate accurately due to the pointy shape of the dilution traces.

Last, the optical coefficients of the blood were chosen to correspond to blood hemoglobin 100% saturated in oxygen. The excitation (784 nm) and emission wavelengths (830 nm) used in the simulations correspond to the peak of absorption and fluorescence emission of ICG. These wavelengths are near the isobestic point of hemoglobin (805 nm) such that the absorption characteristics of hemoglobin vary only by a small amount with O_2 saturation for wavelengths between 784 and 830 nm (Ref. 17). Thus, the simulation results should remain largely valid even for blood that is not fully saturated in oxygen.

5 Conclusions

This study quantified the variations of ICG fluorescence emission and diffusely scattered light simulated or experimentally measured from blood with different hematocrit levels and containing varying amounts of ICG. The results established that measurements of fluorescence and diffusely scattered excitation light could be combined to derive calibration equations relating the blood ICG concentration to these optical measurements. The calibration equations were valid over the wide range of hematocrit levels that can be expected in end-stage renal failure patients receiving hemodialysis. The development of a "universal" calibration obviates the need for serial blood sampling, since once a probe is calibrated, the calibration should be valid across patients and across time. Results from this study will serve in the development of non-invasive measurements systems for hemodynamic parameters including cardiac output and circulating blood volume in patients receiving hemodialysis with the goal of preventing or minimizing intradialytic hypovolemia.

Acknowledgments

Support was provided by the Alfred E. Mann Institute for Biomedical Engineering at the University of Southern California. The authors thank Alan Eskovitz, PhD, for helpful discussions in the interpretation of the data and for his contribution in the design of the optical probe.

References

1. J. T. Daugirdas, "Dialysis hypotension: a hemodynamic analysis," *Kidney Int.* **39**(2), 233–246 (1991).
2. J. K. Leypoldt, A. K. Cheung, R. R. Steuer, D. H. Harris, and J. M. Conis, "Determination of circulating blood volume by continuously monitoring hematocrit during hemodialysis," *J. Am. Soc. Nephrol.* **6**(2), 214–219 (1995).
3. D. Boon, G. A. van Montfrans, M. G. Koopman, R. T. Krediet, and W. J. Bos, "Blood pressure response to uncomplicated hemodialysis: the importance of changes in stroke volume," *Nephron* **96**(3), c82–c87 (2004).
4. S. Mitra, P. Chamney, R. Greenwood, and K. Farrington, "Serial determinations of absolute plasma volume with indocyanine green during hemodialysis," *J. Am. Soc. Nephrol.* **14**(9), 2345–2351 (2003).
5. T. Iijima, T. Aoyagi, Y. Iwao, J. Masuda, M. Fuse, N. Kobayashi, and H. Sankawa, "Cardiac output and circulating blood volume analysis by pulse dye-densitometry," *J. Clin. Monit* **13**, 81–89 (1997).

6. J. M. Maarek, D. P. Holschneider, J. Yang, S. N. Pniak, and E. H. Rubinstein, "Transcutaneous fluorescence dilution cardiac output and circulating blood volume during hemorrhagic hypovolemia," *Anesthesiology* **102**(4), 774–782 (2005).
7. J. M. Maarek, D. P. Holschneider, and E. H. Rubinstein, "Fluorescence dilution technique for measurement of cardiac output and circulating blood volume in healthy human subjects," *Anesthesiology* **106**(3), 491–498 (2007).
8. S. G. Sakka, K. Reinhart, K. Wegscheider, and A. Meier-Hellmann, "Comparison of cardiac output and circulatory blood volumes by transpulmonary thermo-dye dilution and transcutaneous indocyanine green measurement in critically ill patients," *Chest* **121**, 559–565 (2002).
9. T. Imai, K. Takahashi, H. Fukura, and Y. Morishita, "Measurement of cardiac output by pulse dye densitometry using indocyanine green: a comparison with the thermodilution method," *Anesthesiology* **87**, 816–822 (1997).
10. P. Lund-Johansen, "The dye dilution method for measurement of cardiac output," *Eur. Heart J.* **11**, 6–12 (1990).
11. A. Roggan, M. Friebel, K. Dorschel, A. Hahn, and G. Muller, "Optical properties of circulating human blood in the wavelength range 400–2500 nm," *J. Biomed. Opt.* **4**, 36–46 (1999).
12. T. Desmettre, J. M. Devoisselle, and S. Mordon, "Fluorescence properties and metabolic features of indocyanine green (ICG) as related to angiography," *Surv. Ophthalmol.* **45**, 15–27 (2000).
13. J. M. Maarek, D. P. Holschneider, and J. Harimoto, "Fluorescence of indocyanine green in blood: intensity dependence on concentration and stabilization with sodium polyaspartate," *J. Photochem. Photobiol., B* **65**, 157–164 (2001).
14. L. Wang, S. L. Jacques, and L. Zheng, "MCML—Monte Carlo modeling of light transport in multi-layered tissues," *Comput. Methods Programs Biomed.* **47**(2), 131–146 (1995).
15. L. Wang and S. L. Jacques, "Monte Carlo modeling of light transport in multi-layered tissues in standard C," (1992), http://omlc.ogi.edu/software/mc/.
16. D. E. Hyde, T. J. Farrell, M. S. Patterson, and B. C. Wilson, "A diffusion theory model of spatially resolved fluorescence from depth-dependent fluorophore concentrations," *Phys. Med. Biol.* **46**(2), 369–383 (2001).
17. S. A. Prahl, "Optical properties spectra," http://omlc.ogi.edu/spectra/ (accessed 2008).
18. W. F. Cheong, S. A. Prahl, and A. J. Welch, "A review of the optical properties of biological tissues," *IEEE J. Quantum Electron.* **26**, 2166–2185 (1990).
19. M. L. Landsman, G. Kwant, G. A. Mook, and W. G. Zijlstra, "Light-absorbing properties, stability, and spectral stabilization of indocyanine green," *J. Appl. Physiol.* **40**, 575–583 (1976).
20. R. C. Benson and H. A. Kues, "Fluorescence properties of indocyanine green as related to angiography," *Phys. Med. Biol.* **23**, 159–163 (1978).
21. P. R. van den Biesen, F. H. Jongsma, G. J. Tangelder, and D. W. Slaaf, "Yield of fluorescence from indocyanine green in plasma and flowing blood," *Ann. Biomed. Eng.* **23**, 475–481 (1995).
22. R. Weersink, M. S. Patterson, K. Diamond, S. Silver, and N. Padgett, "Noninvasive measurement of fluorophore concentration in turbid media with a simple fluorescence/reflectance ratio technique," *Appl. Opt.* **40**, 6389–6395 (2001).
23. K. R. Diamond, M. S. Patterson, and T. J. Farrell, "Quantification of fluorophore concentration in tissue-simulating media by fluorescence measurements with a single optical fiber," *Appl. Opt.* **42**(13), 2436–2442 (2003).
24. K. R. Diamond, P. P. Malysz, J. E. Hayward, and M. S. Patterson, "Quantification of fluorophore concentration *in vivo* using two simple fluorescence-based measurement techniques," *J. Biomed. Opt.* **10**(2), 024007 (2005).